Testing a Linear Relation: Short-Range Correlations and the EMC Effect for Gluons and Quarks in Nuclei*

Xiao Liang (梁霄)[1†] Chun-Yuan Li (李春园)[1‡] Bin-Peng Shang (尚滨鹏)[1§] Zong-Guo Si (司宗国)[2♮]
Hong-Xin Wang (王宏昕)[2♯] Xing-Hua Yang (杨兴华)[1¶] Dai-Xing Zhang (张代兴)[1♭]

[1]School of Physics and Optoelectronic Engineering, Shandong University of Technology, Zibo, Shandong 255000, China
[2]School of Physics, Shandong University, Jinan, Shandong 250100, China

Abstract: A dark photon is an Abelian gauge boson arising from a new $U(1)_D$ gauge symmetry, coupled to the Standard Model through kinetic mixing. The mixing parameter ϵ induces an effective coupling to the electromagnetic current, while g_χ couples the dark photon to a stable dark matter particle χ. We study J/ψ two-body and four-body decays mediated by a light dark photon ($m_U < 3.0$ GeV) within the non-relativistic QCD (NRQCD) framework, considering both visible decays of the dark photon into SM fermions and invisible decays into dark sector particles. We investigate the detection sensitivity of BESIII and STCF experiments to the dark photon mass m_U and kinetic mixing parameter ϵ. Our results show that, for two-body final states with $m_U < 2m_\chi$, BESIII sets ϵ upper limits of 9.3×10^{-4} and 7.6×10^{-4} for lepton-pair and hadronic signals, respectively, while STCF yields 3.7×10^{-4} and 3.1×10^{-4}. For invisible decays ($m_U \geq 2m_\chi$), BESIII achieves an ϵ limit of 1.4×10^{-3} in the mass range $0.3 \sim 0.8$ GeV, and STCF reaches 2.3×10^{-4} in $0.3 \sim 1.9$ GeV; no signals are expected in other mass regions, and visible decays are severely suppressed throughout. For four-body decay channels, BESIII yields an ϵ upper limit of 7.6×10^{-5} for $m_U < 2.2$ GeV, whereas STCF achieves 1.2×10^{-5} over the full mass range. When $m_U \geq 2m_\chi$, visible modes are nearly excluded; BESIII and STCF set ϵ limits from invisible decays of 8.8×10^{-5} for $m_U < 2.4$ GeV and 1.4×10^{-5} for $m_U < 2.8$ GeV, respectively, with no detectable signals at higher masses. Except for the limit of 9.3×10^{-4}, all the above ϵ bounds lie in regions that are not currently excluded by collider experiments. Compared with the constraints from two-body final state processes, the limits derived from four-body decay channels lie well below existing experimental bounds, providing supportive references for constraining this parameter in BESIII and STCF experiments. Numerical results for the decay ratios $\Gamma/\Gamma_{J/\psi}$, expected event numbers, significance $S/\sqrt{B}$, and p_T distributions are presented where applicable.

Keywords: dark photon, dark matter, NRQCD, J/ψ decay

DOI: 10.1088/1674-1137/ae76fa **CSTR:**

I. INTRODUCTION

Observations of the cosmic microwave background, large-scale structure, and other cosmological probes imply that roughly one quarter of the total energy density of the Universe resides in a non-luminous, non-baryonic component that interacts predominantly via gravity [1]. This makes dark matter (DM) an essential ingredient of the standard cosmological model, even though its nature remains unexplained in the Standard Model (SM) of elementary particle physics. Extensive experimental searches have so far yielded only null or non-reproducible results.

A minimal and well-motivated framework assumes a

Received 21 April 2026; Accepted 3 June 2026

* This work is supported in part by the National Natural Science Foundation of China (12105162, 12305106, 12235008, 12321005), the Natural Science Foundation of Shandong Province (ZR2021QA058, ZR2021QA040), and the Youth Innovation Technology Project of Higher School in Shandong Province (2023KJ146)

† E-mail: lx321@sdut.edu.cn
‡ E-mail: lichunyuan@sdut.edu.cn
§ E-mail: shangbp@sdut.edu.cn
♮ E-mail: zgsi@sdu.edu.cn
♯ E-mail: wanghx@mail.sdu.edu.cn
¶ E-mail: yangxinghua@sdut.edu.cn
♭ E-mail: 24412011130@stumail.sdut.edu.cn

simple $U(1)_D$ gauge symmetry for the dark sector. The associated gauge boson couples to the SM sector through kinetic mixing with the $U(1)_Y$ hypercharge symmetry, effectively introducing a feeble interaction between the dark sector and the SM [2–5]. For dark photon searches, three main methods are employed [2, 6, 7]: a bump hunt in the visible final-state invariant-mass distribution for dark photon decays into SM particles (BaBar [8], Belle [9], KLOE [10], APEX [11], A1 [12]), a missing-energy/momentum search for decays into invisible dark matter (NA64 [13, 14], BaBar [15], Belle II [16], LDMX [17]), and displaced-vertex detection for long-lived dark photons (HPS [18], LHCb [19, 20]). In this work, we focus on the first two approaches.

The theoretically allowed range of the kinetic mixing parameter ϵ is 10^{-7}–10^{-2}, which is consistent with precision electroweak data and remains accessible to dedicated experimental searches. Meanwhile, ongoing improvements in experimental precision have gradually constrained the parameter space in the (m_U, ϵ^2) plane; the most stringent exclusion limits have been set by BaBar [8, 21, 22], LHCb [23, 24], Belle [9], Belle II [16], KLOE [10, 25–27], and CMS [28]. In the dark photon mass range considered in this work, BaBar observed no significant excess between 0.02 GeV and 10.2 GeV, and set upper limits on the mixing strength at the 10^{-4}–10^{-3} level [8]. The Belle Collaboration searched for a dark photon and a dark Higgs boson in the mass ranges 0.1–3.5 GeV/c^2 and 0.2–10.5 GeV/c^2, respectively, and excluded mixing parameter values above 8×10^{-4} [9].

To date, several experiments have searched for dark matter via hadronic decays. For example, the LHCb collaboration proposed a search for dark photons using charm meson decays [19]. In this work, we study the dark sector in J/ψ decays mediated by a dark photon, where J/ψ is a charmonium state composed of a $c\bar{c}$ quark-antiquark pair. Heavy quarkonium systems provide an exceptionally clean environment for probing dark-sector interactions with heavy quarks. The decay of a heavy quark-antiquark bound state is sensitive to dark-sector particles of arbitrarily low mass, making radiative quarkonium transitions a key probe of sub-GeV dark matter [29]. Moreover, extensive experimental data on J/ψ decays are currently available, including 8.774×10^{10} J/ψ events accumulated by the BESIII experiment [30], and the future Super Tau-Charm Facility (STCF) is designed to achieve 3.4×10^{12} J/ψ events per year [31]. Consequently, J/ψ radiative decays provide a realistic and powerful platform for exploring invisible dark-sector signatures.

In this paper, we study J/ψ decays into two-body and four-body final states mediated by a dark photon, aiming to investigate the dark sector. To describe the J/ψ state, we adopt the nonrelativistic QCD (NRQCD) factorization formalism developed by Bodwin, Braaten, and Lepage [32, 33], which is now widely used in phenomenological studies of quarkonium production and decay. In the NRQCD factorization formalism, quarkonium production and decay amplitudes can be separated into short-distance coefficients and long-distance matrix elements. The short-distance coefficients describe the perturbative annihilation (or production) of the heavy-quark pair, while the long-distance matrix elements characterize the nonperturbative hadronization of the heavy-quark pair into the physical quarkonium state.

Significant progress has been made in dark-sector phenomenology, using a variety of processes as documented in the literature. For instance, dark photon searches using $e^+e^-\to\gamma A'\to\gamma\mu^+\mu^-$ at future e^+e^- colliders (CEPC, ILC, and FCC-ee) were studied in Ref. [34]. The pair production of dark photons, $e^+e^-\to A'A'$ with each A' decaying to a muon pair, has also been studied at future e^+e^- colliders (CEPC, FCC-ee, ILC/ILD, and IDEA) [35]. Based on a parametrised simulation of the IDEA detector, Ref. [36] studied the production of a dark photon at the proposed CERN FCC-ee collider. In Ref. [37], our group discussed the production of a vector dark photon and a scalar mediator in the process $e^+e^-\to q\bar{q}A'$ via electron-positron collisions. Ref. [38] investigates the sensitivity of CEPC and FCC-ee at 240 GeV to long-lived dark photons above 2 GeV that are pair-produced via a light scalar mixing with the Higgs boson. The search for massless dark photons via decays of the charmed pseudoscalar mesons D^+, D^0, and D_s^+, and the singly charmed baryons Λ_c^+, Ξ_c^+, and Ξ_c^0, is investigated in Ref. [39]. Ref. [40] explored massless dark photons via two-body hyperon decays. Ref. [41] analyzed the flavor-changing neutral-current (FCNC) process $f\to f'\gamma'$, in which a fermion f decays to a lighter fermion f' and a massless dark photon. In addition, the phenomenology of the dark Z boson at the International Linear Collider was studied in Ref. [42].

In this manuscript, we calculate the two-body and four-body decay processes of J/ψ mediated by a light dark photon ($m_U < 3.0$ GeV). We discuss both decays of the dark photon into visible Standard Model particles and its decays into invisible dark-sector particles, including Dirac fermions, Majorana fermions, and complex scalar particles. To make our work more useful for experimental studies, we focus on the numerical results for the decay width ratios $\Gamma/\Gamma_{J/\psi}$ and the expected event numbers at BESIII. In addition, the significance $S/\sqrt{B}$ and the transverse momentum p_T distributions are studied where appropriate.

The rest of the paper is organized as follows. In Section II, the main theoretical framework of the dark sector and J/ψ decays are presented. In Section III, our comprehensive numerical results are discussed. Section IV concludes with a summary.

II. FORMULATION

A. J/ψ decay

Within the NRQCD framework, the differential decay rate of the process $J/\psi \to l^+l^-U$ can be factorized into the short-distance coefficients and the long-distance matrix elements. The short-distance coefficients are obtained perturbatively from Feynman diagram calculations. The Feynman diagrams and their amplitudes are generated using FeynArts [43]. Subsequently, we employ FeynCalc [44] to evaluate Dirac traces and perform Lorentz tensor algebra. At leading order in the relative velocity expansion, the projection of the heavy quark pair $(c\bar{c})$ onto the J/ψ state is performed by the replacement [32, 33],

$$\Pi_p = \epsilon_\alpha \frac{1}{2\sqrt{M}} \gamma^\alpha (\not{p} + M) \otimes \frac{\delta_{ij}}{\sqrt{N_c}} , \tag{1}$$

where p and ϵ_α are the momentum and polarization vector of the J/ψ, respectively. δ_{ij} ensures the color-singlet nature of the J/ψ, and $N_c = 3$ is the number of quark colors. When evaluating the squared amplitudes $|\mathcal{M}|^2$, we need to sum over the polarization vectors of the J/ψ; the prescription for this sum is given in [33]

$$\sum \epsilon_\alpha \epsilon_{\alpha'} = \Pi_{\alpha\alpha'} = -g^{\alpha\alpha'} + \frac{p^\alpha p^{\alpha'}}{M^2} . \tag{2}$$

While long-distance matrix elements are non-perturbative and expressed in terms of universal parameters, these elements are determined by the squared Schrödinger wavefunction at the origin $|\Psi(r=0)|^2$, which is related to the radial wavefunction $R_n(r=0)$.

$$\langle 0|\mathcal{O}^{J/\psi}|0\rangle = |\Psi_{J/\psi}(r=0)|^2 = \frac{|R_{J/\psi}(r=0)|^2}{4\pi} , \tag{3}$$

Such matrix elements can be determined using approaches including lattice QCD calculations [45], potential models [46], and experimental measurements. In the present work, we adopt the experimental extraction approach to obtain the value of $|R_{J/\psi}(r=0)|^2$.

B. Lagrangian of dark photon

Renormalizable portals provide a compelling framework for connecting a dark sector to the Standard Model (SM) [2–5]. These correspond to dimension-four operators that couple SM fields to new gauge-singlet degrees of freedom. In this work, we focus on the vector portal, in which a new Abelian $U(1)_D$ gauge symmetry kinetically mixes with the hypercharge $U(1)_Y$ [2, 47–49]. The Lagrangian of the relevant gauge terms is

$$\mathcal{L} \supset -\frac{1}{4}\hat{B}_{\mu\nu}\hat{B}^{\mu\nu} - \frac{1}{4}\hat{Z}_{D\mu\nu}\hat{Z}_D^{\mu\nu} + \frac{1}{2}\frac{\epsilon}{\cos\theta}\hat{Z}_{D\mu\nu}\hat{B}^{\mu\nu} + \frac{1}{2}m_{D,0}^2\hat{Z}_D^\mu\hat{Z}_{D\mu} . \tag{4}$$

The quantities $\hat{B}_{\mu\nu}$ and $\hat{Z}_{D\mu\nu}$ denote the field strength tensors of $U(1)_Y$ and $U(1)_D$, respectively. θ is the Weinberg mixing angle, and ϵ is the kinetic mixing parameter. After electroweak symmetry breaking, the dark photon mixes with two neutral gauge bosons—the photon and the Z^0. The gauge-kinetic mixing term in the Lagrangian is $\mathcal{L} \supset \frac{\epsilon}{2} B_{\mu\nu} Z_D^{\mu\nu}$. In the following, we use A'_μ to denote this dark photon field and m_U to represent its mass. The leading-order couplings of the dark photon to fermions are proportional to ϵ and depend on the ratio m_U/m_Z. For $\epsilon \ll 1$ and $m_U \ll m_Z$, the couplings are photon-like. In our study, we restrict the dark photon mass to $m_U \leq 3$ GeV, so that the mixing with the Z^0 boson is negligible, and the photon-like coupling approximation is well justified. After diagonalizing the gauge-kinetic and mass mixing terms, the dominant low-energy effective interaction is given by $\epsilon e A'_\mu J^\mu_{\rm EM}$. Therefore, the Lagrangian for the dark photon coupling to SM particles is

$$\mathcal{L} \supset \epsilon e\, x_f A'_\mu J^\mu_{\rm EM} , \tag{5}$$

where $x_l = -1$, $x_\nu = 0$, and $x_q = 2/3$ or $-1/3$ for quarks. The specific forms of the Lagrangian are

$$\mathcal{L} \supset \epsilon e\, x_f A'_\mu J^\mu_{\rm EM} = \begin{cases} -\epsilon e A'_\mu \bar{l}\gamma^\mu l , & \\ \frac{2}{3}\epsilon e A'_\mu \bar{q}_i \gamma^\mu q_i & q_i = u, c , \\ -\frac{1}{3}\epsilon e A'_\mu \bar{q}_i \gamma^\mu q_i & q_i = d, s, b . \end{cases} \tag{6}$$

Under the new Abelian $U(1)_D$ gauge symmetry, the dark photon interacts with the stable dark matter (DM) particle χ via the dark gauge coupling g_χ.

$$\mathcal{L} \supset -g_\chi A'_\mu J^\mu_\chi . \tag{7}$$

The form of the dark current J^μ_χ depends on the spin of the dark-sector state and can be classified into Dirac fermion, Majorana fermion, and complex scalar dark matter cases. The corresponding Lagrangian has the form [50]

$$\mathcal{L} \supset -g_\chi A'_\mu J^\mu_\chi = \begin{cases} -g_\chi A'_\mu \bar{\chi}_D \gamma^\mu \chi_D & \text{Dirac fermion} , \\ -\frac{1}{2} g_\chi A'_\mu \bar{\chi}_M \gamma^\mu \gamma^5 \chi_M & \text{Majorana fermion} , \\ -i g_\chi A'_\mu \left(\varphi^\dagger \partial^\mu \varphi - (\partial^\mu \varphi^\dagger)\varphi\right) & \text{complex scalar} . \end{cases} \tag{8}$$

The mass terms for the three types of dark matter in

the Lagrangian are

$$\mathcal{L}^{X}_{\rm mass} = \begin{cases} -m_\chi \bar{\chi}_D \chi_D & \text{Dirac fermion ,} \\ -\frac{1}{2} m_\chi \bar{\chi}_M \chi_M & \text{Majorana fermion ,} \\ -m_\chi^2 \varphi^\dagger \varphi & \text{complex scalar .} \end{cases} \tag{9}$$

In this work, we consider all these dark matter candidates.

C. Two body final state decay of J/ψ

In this work, we discuss the two-body final-state decay of J/ψ mediated by a dark photon. A representative Feynman diagram is shown in Fig. 1(1). The decay processes are governed by the visible width for decays into SM states and the invisible width for decays into dark states.

$$\Gamma_{\rm total} = \begin{cases} \Gamma_{\rm vis} & m_U < 2m_\chi \,, \\ \Gamma_{\rm vis} + \Gamma_{\rm inv} & m_U \geq 2m_\chi \,. \end{cases} \tag{10}$$

Here m_U is the mass of the dark photon, which can be generated via either a Stueckelberg term or a dark Higgs mechanism [48, 51−55]. The form of $\Gamma_{\rm vis}$ becomes[1)]

$$\Gamma_{\rm vis}(m_U) = \sum_{l=e,\mu} \Gamma(J/\psi \to U \to l^+ l^-) + \Gamma(J/\psi \to U \to \text{hadrons}) \,, \tag{11}$$

The decay width of the dark photon into hadrons is incorporated via a global R-ratio,

$$\Gamma(J/\psi \to U \to \text{hadrons}) = R(\sqrt{s})\, \Gamma(J/\psi \to U \to \mu^+\mu^-) \,, \tag{12}$$

where we use the ratio $R(\sqrt{s}) = \sigma_{e^+e^-\to\text{hadrons}}/\sigma_{e^+e^-\to\mu^+\mu^-}$, with $\sqrt{s}$ denoting the center-of-mass energy of the reaction system [56, 57]. For the two-body final-state decay, the dark photon is off-shell, so $R(\sqrt{s}) = R(M_{J/\psi})$. Ref. [58] presents the measurement of the R ratio in the energy range from 1.84 GeV to 3.72 GeV at the KEDR detector. From these results, we deduce $R(M_{J/\psi}) = 2.16$. The form of $\Gamma_{\rm inv}$ is

$$\Gamma_{\rm inv}(m_U) = \sum_{l=\chi_D,\chi_M,\varphi} \Gamma(J/\psi \to U \to \bar{\chi}\chi) \,. \tag{13}$$

In the calculation, the total decay width Γ_U of the dark photon is approximated as the sum of two-body final-state processes. To satisfy this condition and improve accuracy, we choose dark photon masses well separated from the $2m_e$ and $2m_\mu$ thresholds. We therefore select masses in the range 0.3–3 GeV.

D. Four body final state decay of J/ψ

We study the four-body final-state decay $J/\psi \to l^+l^- U \to l^+l^- X$. A representative Feynman diagram is shown in Fig. 1, panel (2). The decay width of the total process can be decomposed into

$$\Gamma(J/\psi \to l^+l^- U \to l^+l^- X) = \Gamma(J/\psi \to l^+l^- U) \times \text{Br}(U \to X) \,. \tag{14}$$

Here, the branching ratio $\text{Br}(U \to X)$ accounts for visible decays $\text{Br}(U \to e^+e^-)$, $\text{Br}(U \to \mu^+\mu^-)$, and $\text{Br}(U \to \text{hadrons})$, as well as invisible decays $\text{Br}(U \to \bar{\chi}_D\chi_D)$, $\text{Br}(U \to \bar{\chi}_M\chi_M)$, and $\text{Br}(U \to \varphi^\dagger\varphi)$. It takes the form

$$\text{Br}(U \to X) = \begin{cases} \dfrac{\Gamma(U \to X)}{\Gamma_{\rm vis}} & m_U < 2m_\chi \,, \\ \dfrac{\Gamma(U \to X)}{\Gamma_{\rm vis} + \Gamma_{\rm inv}} & m_U \geq 2m_\chi \,. \end{cases} \tag{15}$$

Here $\Gamma_{\rm vis}$ and $\Gamma_{\rm inv}$ are [2)]

$$\begin{aligned} \Gamma_{\rm vis}(m_U) &= \sum_{l=e,\mu} \Gamma(U \to l^+l^-) + \Gamma(U \to \text{hadrons}) \,, \\ \Gamma_{\rm inv}(m_U) &= \sum_{l=\chi_D,\chi_M,\varphi} \Gamma(U \to \bar{\chi}\chi) \,, \end{aligned} \tag{16}$$

where

$$\Gamma(U \to \text{hadrons}) = R(\sqrt{s})\, \Gamma(U \to \mu^+\mu^-). \tag{17}$$

For the four-body final-state decay, the dark photon we consider is on shell. Therefore, the center-of-mass energy $\sqrt{s}$ is equivalent to the on-shell dark photon mass m_U, leading to $R(\sqrt{s}) = R(m_U)$. Using the data from PDG2024 [29], we extract $R(m_U)$ in the mass range $2m_\mu \leq m_U < M_{J/\psi}$ and present the results in Fig. 2.

1) The explicit expressions for the decay widths $\Gamma(J/\psi \to U \to l^+l^-)$, $\Gamma(J/\psi \to U \to \bar{\chi}_D\chi_D)$, $\Gamma(J/\psi \to U \to \bar{\chi}_M\chi_M)$, and $\Gamma(J/\psi \to U \to \varphi^\dagger\varphi)$ are presented in Appendix A.

2) The explicit expressions for the squared amplitude of the process $J/\psi \to l^+l^- U$ and the decay widths $\Gamma(U \to l^+l^-)$, $\Gamma(U \to \bar{\chi}_D\chi_D)$, $\Gamma(U \to \bar{\chi}_M\chi_M)$ and $\Gamma(U \to \varphi^\dagger\varphi)$ are presented in Appendix A.

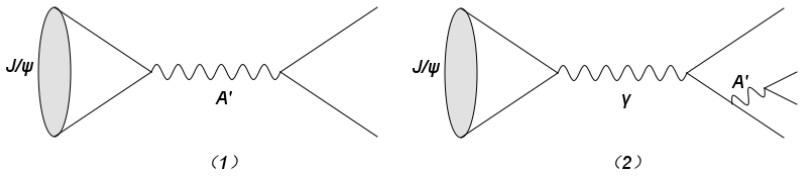

Fig. 1. Typical Feynman diagrams for the decay of J/ψ into a two-body final state (left) and into a four-body final state (right), mediated by a dark photon A'.

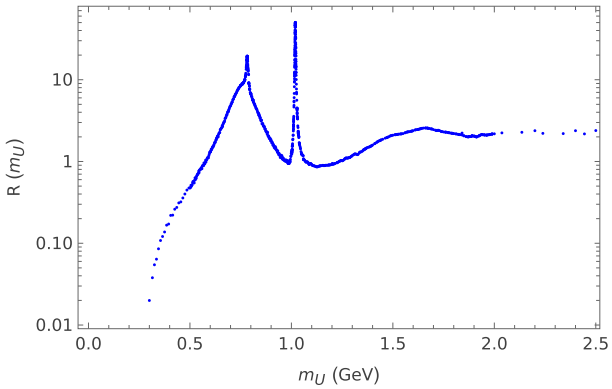

Fig. 2. (color online) The curves depict the parameter $R(m_U)$ as a function of m_U over the mass range $2m_\mu \le m_U < M_{J/\psi}$.

Therefore, the decay branching ratio of the target process is

$$\mathcal{B}(J/\psi \to l^+l^-X) = \frac{\Gamma(J/\psi \to l^+l^-X)}{\Gamma_{J/\psi}} = \frac{\Gamma(J/\psi \to l^+l^-U)}{\Gamma_{J/\psi}} \times \mathrm{Br}(U \to X) , \tag{18}$$

Since we aim to study the dark photon by reconstructing its invariant mass from final-state particles and assume it is produced on-shell without off-shell contributions, the resulting yield is expected to be lower than the directly measured value. Therefore, our prediction can serve as a baseline for future experimental searches.

III. NUMERICAL RESULTS

In the numerical calculations, the input parameters are taken as follows [29]:

$$\alpha = 1/137.065,\ M_{J/\psi} = 3.0969\ \mathrm{GeV},\ \Gamma_{J/\psi} = 92.6\ \mathrm{keV},$$
$$m_e = 0.511\ \mathrm{MeV},\ m_\mu = 0.106\ \mathrm{GeV} .$$

To determine the value of the J/ψ radial wavefunction at the origin, we use the experimental branching ratios $\Gamma(J/\psi \to e^+e^-)/\Gamma_{J/\psi}$ and $\Gamma(J/\psi \to \mu^+\mu^-)/\Gamma_{J/\psi}$, and extract its value from their average for our two subsequent numerical evaluations. We obtain

$$|R_{J/\psi}(0)|^2 = 0.5599\ \mathrm{GeV}^3 .$$

For the dark coupling α_χ, a larger α_χ leads to a larger dark matter annihilation cross-section, thereby reducing the relic density. In the thermal freeze-out mechanism, α_χ, ϵ, and m_U determine the annihilation cross-section required to match the observed dark matter relic density. In this work, we adopt a theoretically reasonable benchmark value $\alpha_\chi = 0.05$, where

$$\alpha_\chi = \frac{g_\chi^2}{4\pi} = 0.05 .$$

A. two-body final-state decay of J/ψ mediated by the dark photon

(I) $m_U < 2m_\chi$

When $m_U < 2m_\chi$, only visible decays occur. In Fig. 3, we display the decay width as a function of the kinetic mixing parameter ϵ for the visible decay processes $J/\psi \to U \to e^+e^-$, $J/\psi \to U \to \mu^+\mu^-$, and $J/\psi \to U \to$ hadrons, with the dark photon mass fixed at $m_U = 1.0$ GeV as an example. We also show the experimental limits for BESIII and STCF. According to the BESIII experiment, the total number of J/ψ events is 8.774×10^{10} with a luminosity of about 2568.07 pb^{-1} [59]. The STCF experiment is designed to achieve 3.4×10^{12} J/ψ events with an instantaneous luminosity greater than 0.5×10^{35} $\mathrm{cm}^{-2}\mathrm{s}^{-1}$ [31]. For BESIII, no lepton or hadron signals can be detected when ϵ is below approximately 9.3×10^{-4} and 7.6×10^{-4}, respectively, while these ϵ limits can be further lowered to 3.7×10^{-4} and 3.1×10^{-4} at STCF, for the entire mass range 0.3 GeV $\le m_U \le$ 3.0 GeV. Our theoretical prediction for the ratio of muon pair production to electron pair production is:

$$\frac{\Gamma(J/\psi \to U \to \mu^+\mu^-)}{\Gamma(J/\psi \to U \to e^+e^-)} = 0.999992 .$$

We then fix the coupling parameter to $\epsilon = 10^{-3}$ as an example and analyze the event yields and kinematic distributions at BESIII and STCF. In Fig. 4, we display the decay width as a function of the dark photon mass m_U. In addition, we adopt several typical mass values,

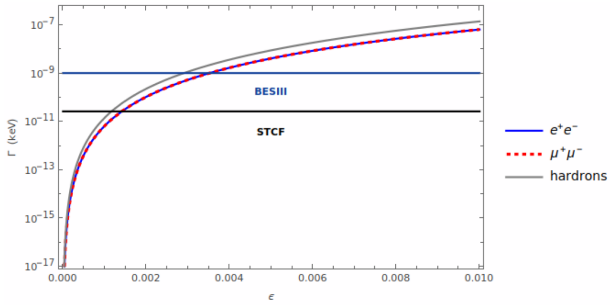

Fig. 3. (color online) Decay widths as functions of the kinetic mixing parameter ϵ for the visible decay processes $J/\psi \to U \to e^+e^-$, $J/\psi \to U \to \mu^+\mu^-$, and $J/\psi \to U \to$ hadrons, with $m_U = 1.0$ GeV. The dark blue and black horizontal lines represent the experimental limits from BESIII and STCF, respectively.

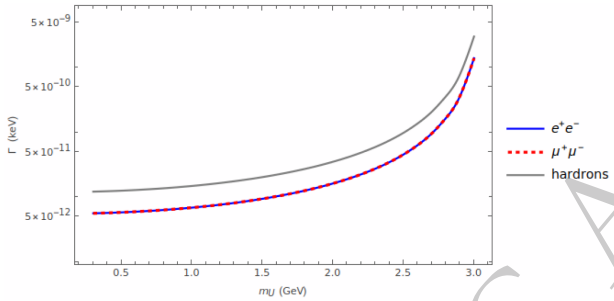

Fig. 4. (color online) Decay width as a function of the dark photon mass m_U for the visible decay processes $J/\psi \to U \to e^+e^-$, $J/\psi \to U \to \mu^+\mu^-$, and $J/\psi \to U \to$ hadrons, with $\epsilon = 10^{-3}$.

$m_U = \{0.5, 1.0, 1.5, 2.0, 2.5\ \text{GeV}\}$, and list their corresponding decay ratios $\Gamma/\Gamma_{J/\psi}$ in Table 1. The results for all processes exhibit an overall increase with increasing m_U. This behavior arises primarily because Γ is approximately proportional to $1/(m_U^2 - M_{J/\psi}^2)^2$. Here we neglect the term $m_U^2\Gamma_U^2$ because $\Gamma_U = \Gamma_{vis}$ is directly proportional to ϵ^2, rendering $m_U^2\Gamma_U^2$ negligibly small.

As shown in the figure, after accounting for the BESIII detection efficiencies of 59.21% and 63.53% for J/ψ decaying into e^+e^- and $\mu^+\mu^-$, respectively [60], the observed signal yield is almost negligible. However, at the STCF, the expected event yields for the dark photon mediated $J/\psi \to e^+e^-$ (and similarly $J/\psi \to \mu^+\mu^-$) are about $0 \sim 51$ in the mass range $2.3\ \text{GeV} \le m_U \le 3.0\ \text{GeV}$, while for $J/\psi \to$ hadrons they are about $0 \sim 110$ in the range $1.8\ \text{GeV} \le m_U \le 3.0\ \text{GeV}$.

Using the $J/\psi \to e^+e^-$ decay channel as an example, we estimate the significance $S/\sqrt{B}$ to be less than 1.132×10^{-4} at the STCF. This estimate uses the background branching ratio $\mathcal{B}(J/\psi \to e^+e^-) = 5.971\%$ from PDG2024 [29]. Such a small significance indicates that

Table 1. Predictions for the decay ratios $\Gamma/\Gamma_{J/\psi}$ of the visible two-body decay process for $m_U = \{0.5, 1.0, 1.5, 2.0, 2.5, 3.0\ \text{GeV}\}$ with $\epsilon = 10^{-3}$. The theoretical uncertainty is entirely due to the experimental uncertainty in the J/ψ mass.

$\mathcal{B}(\times 10^{-13})$	e^+e^-	$\mu^+\mu^-$	hadrons	$\Gamma_{vis}/\Gamma_{J/\psi}$
0.5 GeV	0.629 ± 0.0113	0.629 ± 0.0113	1.359 ± 0.0245	2.616 ± 0.0472
1.0 GeV	0.744 ± 0.0134	0.744 ± 0.0134	1.606 ± 0.0290	3.093 ± 0.0558
1.5 GeV	1.0183 ± 0.0184	1.0183 ± 0.0184	2.200 ± 0.0397	4.236 ± 0.0764
2.0 GeV	1.755 ± 0.0316	1.755 ± 0.0316	3.792 ± 0.0684	7.303 ± 0.132
2.5 GeV	4.913 ± 0.0886	4.913 ± 0.0886	10.612 ± 0.191	20.437 ± 0.368

firm control of statistical and systematic issues is necessary to obtain reliable results. We predict that increasing the event yield of J/ψ by two orders of magnitude will lead to a corresponding increase in all significances by one order of magnitude.

Finally, we perform a more essential phenomenological analysis for the visible decay process $J/\psi \to U \to e^+e^-$ as an example [1)]. Fig. 7 displays the transverse momentum p_T distributions of the decay width for various dark photon masses. It is found that the distributions rise sharply as m_U increases.

(II) $m_U \ge 2m_\chi$

When $m_U \ge 2m_\chi$, visible and invisible decays occur simultaneously. In the corresponding experiments, the presence of invisible decays may be inferred from a resonance-like feature in the missing-mass or missing-momentum distribution with a single photon. In Fig. 5, we display the decay width as a function of the kinetic mixing parameter ϵ for the visible decay processes $J/\psi \to U \to e^+e^-$, $J/\psi \to U \to \mu^+\mu^-$ and $J/\psi \to U \to$ hadrons, as well as the invisible decay processes $J/\psi \to U \to \bar{\chi}_D\chi_D$, $J/\psi \to U \to \bar{\chi}_M\chi_M$ and $J/\psi \to U \to \varphi^\dagger\varphi$, with the dark photon mass fixed to $m_U = 1.0$ GeV as an example. It can be seen that, within the theoretically allowed range of ϵ (10^{-7} to 10^{-2}), all visible decays are excluded at both BESIII and STCF. This is because the visible final states of SM particles are strongly suppressed by the invisible decay channels when $m_U \ge 2m_\chi$. For invisible decays, the ϵ limit is 1.4×10^{-3} for the dark photon mass range $0.3\ \text{GeV} \le m_U \le 0.8\ \text{GeV}$, but for masses above 0.8 GeV, no signals can be detected within the theoretically allowed range of ϵ at BESIII. Meanwhile, the ϵ limit is 2.3×10^{-4} for the dark photon mass range $0.3\ \text{GeV} \le m_U \le 1.9\ \text{GeV}$, but for masses above 1.9 GeV, no signals can be detected at STCF.

By fixing $\epsilon = 10^{-3}$ as an example, we plot the decay width as a function of the dark photon mass m_U for both visible and invisible decay processes, as shown in Fig. 6. We further select a set of typical dark photon masses $m_U = \{0.5, 1.0, 1.5, 2.0, 2.5\ \text{GeV}\}$, with the corresponding

1) The explicit expression for the differential decay width $d\Gamma(J/\psi \to U \to l^+l^-)/dp_T$ is presented in Appendix A.

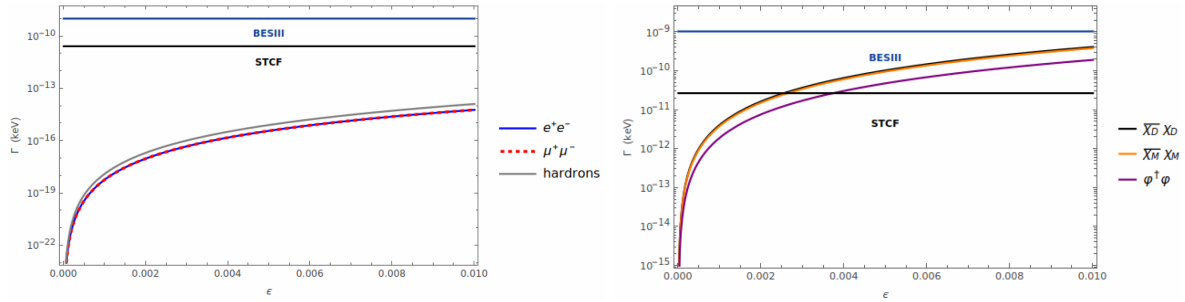

Fig. 5. (color online) Left: Decay width as a function of the kinetic mixing parameter ϵ for the visible decays $J/\psi \to U \to e^+e^-$, $J/\psi \to U \to \mu^+\mu^-$, and $J/\psi \to U \to$ hadrons. The dark blue and black horizontal lines represent the experimental limits from BESIII and STCF, respectively. Right: Decay width as a function of the kinetic mixing parameter ϵ for the invisible decays $J/\psi \to U \to \bar{\chi}_D\chi_D$, $J/\psi \to U \to \bar{\chi}_M\chi_M$, and $J/\psi \to U \to \varphi^\dagger\varphi$, with $\alpha_\chi = 0.05$ and $m_U/m_\chi = 3.0$. Both figures correspond to $m_U = 1.0$ GeV.

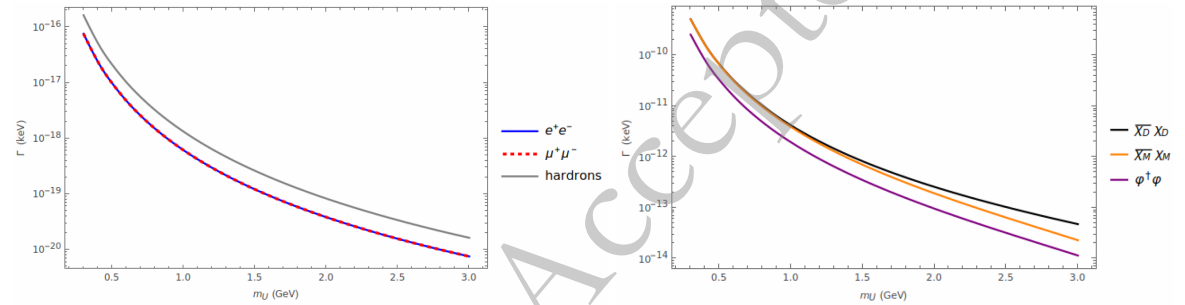

Fig. 6. (color online) Left: Decay width as a function of the dark photon mass m_U for the visible decay processes $J/\psi \to U \to e^+e^-$, $\mu^+\mu^-$, and hadrons. Right: Decay width as a function of the dark photon mass m_U for the invisible decay processes $J/\psi \to U \to \bar{\chi}_D\chi_D$, $\bar{\chi}_M\chi_M$, and $\varphi^\dagger\varphi$, with $\alpha_\chi = 0.05$ and $m_U/m_\chi = 3.0$. In both figures, $\epsilon = 10^{-3}$.

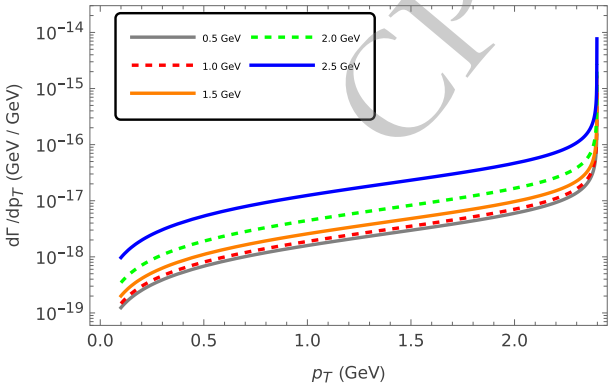

Fig. 7. (color online) The differential cross-section distributions $d\sigma/dp_T$ for the process $J/\psi \to U \to e^+e^-$ for dark photon masses $m_U = \{0.5, 1.0, 1.5, 2.0, 2.5\}$ GeV.

decay ratios $\Gamma/\Gamma_{J/\psi}$ listed in Table 2. It is evident from both the table and the curve that, for both visible and invisible decay channels, the decay width declines sharply as m_U approaches the J/ψ threshold. The main reason for this trend is that Γ contains the denominator $1/[(m_U^2 - M_{J/\psi}^2) + m_U^2\Gamma_U^2]$, and here the value of $\Gamma_U = \Gamma_{vis} + \Gamma_{inv}$, which includes both visible and invisible processes, is relatively large, making Γ directly proportional to $1/(m_U^2\Gamma_U^2)$. For all invisible decay channels combined, the expected event yield remains below ten events at BESIII, whereas it ranges from 0 to 47 at STCF for masses below 0.8 GeV with $\epsilon = 10^{-3}$. Strict management of statistical and systematic uncertainties is required as well.

B. four-body final-state decay of J/ψ mediated by a dark photon

(I) $m_U < 2m_\chi$

In Fig. 8, we show the decay width $\Gamma(J/\psi \to l^+l^-U \to l^+l^-X)$ divided by ϵ^2 as a function of the dark photon mass m_U for $l = e, \mu$ and $X = e^+e^-, \mu^+\mu^-,$ hadrons. Here, $J/\psi \to e^+e^-\mu^+\mu^-$ includes $J/\psi \to e^+e^-U \to e^+e^-\mu^+\mu^-$ and $J/\psi \to \mu^+\mu^-U \to \mu^+\mu^-e^+e^-$. The magnitudes of all processes decrease roughly with m_U up to 3.0 GeV, and the spectral shape of hadronic final-state channels is determined by $R(m_U)$. For masses below 2.2 GeV, signals become undetectable at BESIII when ϵ falls below 7.6×10^{-5}. In the range 2.2 GeV $\le m_U \le$ 3.0 GeV, no detectable signals are expected. The STCF, on the other hand, can push the corresponding ϵ limit down to 1.2×10^{-5} across the full accessible mass range.

We then fix the coupling parameter $\epsilon = 10^{-4}$ as a benchmark for the subsequent analysis. In Table 3, we present the decay width ratio $\Gamma/\Gamma_{J/\psi}$ for dark photon masses $m_U = \{0.5, 1.0, 1.5, 2.0, 2.5\}$ GeV. These results are

Table 2. We present predictions for the decay width ratios $\Gamma/\Gamma_{J/\psi}$ of the two-body final-state invisible decay process for $m_U = 0.5, 1.0, 1.5, 2.0, 2.5, 3.0$ GeV. The theoretical uncertainty originates entirely from the experimental uncertainty in the J/ψ mass. Here $\epsilon = 10^{-3}$ and $\alpha_\chi = 0.05$.

$\mathcal{B}(\times 10^{-19})$	e^+e^-	$\mu^+\mu^-$	hadrons	$\Gamma_{vis}/\Gamma_{J/\psi}$
0.5 GeV	1.0591 ± 0.0191	1.0591 ± 0.0191	2.288 ± 0.0412	4.406 ± 0.0794
1.0 GeV	0.0662 ± 0.00119	0.0662 ± 0.00119	0.143 ± 0.00258	0.275 ± 0.00496
1.5 GeV	0.0131 ± 0.000236	0.0131 ± 0.000236	0.0282 ± 0.000509	0.0544 ± 0.000981
2.0 GeV	0.00414 ± 0.0000746	0.00414 ± 0.0000746	0.00894 ± 0.000161	0.0172 ± 0.000310
2.5 GeV	0.00169 ± 0.0000305	0.00169 ± 0.0000305	0.00366 ± 0.0000660	0.00705 ± 0.000127
$\mathcal{B}(\times 10^{-14})$	$\bar{\chi}_D\chi_D$	$\bar{\chi}_M\chi_M$	$\varphi^\dagger\varphi$	$\Gamma_{inv}/\Gamma_{J/\psi}$
0.5 GeV	72.580 ± 1.308	71.326 ± 1.286	35.663 ± 0.643	179.569 ± 3.237
1.0 GeV	4.533 ± 0.0817	4.225 ± 0.0762	2.112 ± 0.0381	10.870 ± 0.196
1.5 GeV	0.892 ± 0.0161	0.760 ± 0.0137	0.380 ± 0.00685	2.0318 ± 0.0366
2.0 GeV	0.280 ± 0.00504	0.208 ± 0.00376	0.104 ± 0.00188	0.592 ± 0.0107
2.5 GeV	0.112 ± 0.00202	0.0695 ± 0.00125	0.0348 ± 0.000627	0.216 ± 0.00390

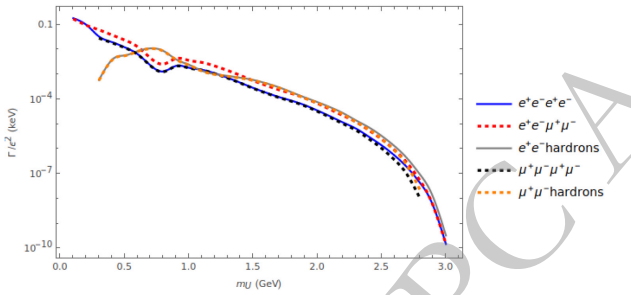

Fig. 8. (color online) Decay width $\Gamma(J/\psi \to l^+l^-U \to l^+l^-X)$ divided by ϵ^2 as a function of the dark photon mass m_U, for the four-body final-state decay processes: $J/\psi \to l^+l^-U \to l^+l^-\mu^+\mu^-$, $J/\psi \to l^+l^-U \to l^+l^-e^+e^-$, and $J/\psi \to l^+l^-U \to l^+l^-$hadrons.

obtained by applying the method outlined in Eq. (18). Based on the J/ψ experimental data at STCF, for m_U below 0.2 GeV the $e^+e^-e^+e^-$ and $e^+e^-\mu^+\mu^-$ final states can yield approximately $37 \sim 64$ and $35 \sim 62$ events, respectively. The corresponding significance $S/\sqrt{B}$ is $2.6\times10^{-3} \sim 4.9\times10^{-3}$ and $3.1\times10^{-3} \sim 5.9\times10^{-3}$, respectively, where the branching ratios of the background processes are $\mathcal{B}(J/\psi \to e^+e^-e^+e^-) = 5.5 \pm 0.5 \times 10^{-5}$ and $\mathcal{B}(J/\psi \to e^+e^-\mu^+\mu^-) = 3.53 \pm 0.26 \times 10^{-5}$ [29]. For such a light dark photon, the only accessible decay channel is e^+e^-. In the mass range 0.2 GeV to 3.0 GeV, the event yields from the final states with two lepton pairs are considerably smaller. For the final state l^+l^- + two jets, the event yield is about 4 near $m_U = 0.78$ GeV and negligible at other masses. Nevertheless, all decay channels yield fewer than 10 events at BESIII.

(II) $m_U \geq 2m_\chi$

In Fig. 9, we fix the dark photon mass to $m_U = 1.0$ GeV and display the decay width as a function of the kinetic mixing parameter ϵ for the four-body final-state visible decay processes $J/\psi \to l^+l^-U \to l^+l^-\mu^+\mu^-$, $J/\psi \to l^+l^-U \to l^+l^-e^+e^-$, and $J/\psi \to l^+l^-U \to l^+l^-$hadrons, as well as the invisible decay processes $J/\psi \to l^+l^-U \to l^+l^-\bar{\chi}_D\chi_D$, $J/\psi \to l^+l^-U \to l^+l^-\bar{\chi}_M\chi_M$, and

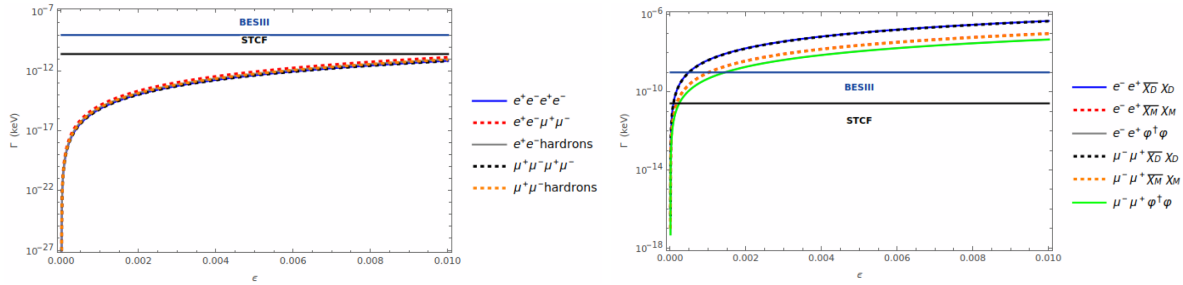

Fig. 9. (color online) Left panel: Decay width as a function of the kinetic mixing parameter ϵ for the visible decay processes $J/\psi \to l^+l^-U \to l^+l^-\mu^+\mu^-$, $J/\psi \to l^+l^-U \to l^+l^-e^+e^-$, and $J/\psi \to l^+l^-U \to l^+l^-$hadrons. The dark blue and black horizontal lines represent the experimental limits from BESIII and STCF, respectively. Right panel: Decay width as a function of the kinetic mixing parameter ϵ for the invisible decay processes $J/\psi \to l^+l^-U \to l^+l^-\bar{\chi}_D\chi_D$, $J/\psi \to l^+l^-U \to l^+l^-\bar{\chi}_M\chi_M$, and $J/\psi \to l^+l^-U \to l^+l^-\varphi^\dagger\varphi$, with $\alpha_\chi = 0.05$ and $m_U/m_\chi = 3.0$. Both panels correspond to $m_U = 1.0$ GeV.

$J/\psi \to l^+l^-U \to l^+l^-\varphi^\dagger\varphi$. Because the visible decay channels are strongly suppressed relative to the invisible ones, they are essentially ruled out by both BESIII and STCF over the theoretically allowed range of ϵ. For invisible decays, the ϵ limit is 8.8×10^{-5} for dark photon masses below 2.4 GeV, whereas for $2.4\,\text{GeV} \le m_U \le 3.0\,\text{GeV}$ no signals can be detected at BESIII within the theoretically allowed range of ϵ. For STCF, the ϵ limit is 1.4×10^{-5} for dark photon masses below 2.8 GeV, while for $m_U > 2.8$ GeV no signals can be detected.

Fixing the coupling parameter $\epsilon = 10^{-4}$ as a benchmark, we evaluate the width of the four-body decay process $J/\psi \to l^+l^-U \to l^+l^-X$ as a function of the dark photon mass m_U, where $l = e, \mu$ and $X = e^+e^-, \mu^+\mu^-$, hadrons, $\bar{\chi}_D\chi_D, \bar{\chi}_M\chi_M, \varphi^\dagger\varphi$. Here we adopt $\alpha_\chi = 0.05$ and $m_U/m_\chi = 3.0$, and present the results in Fig. 10. As shown in the figure, both the visible decay width and the invisible decay width exhibit a roughly decreasing trend with increasing m_U. The behavior of the curves for the four-body final-state decay process is dominated by the process $J/\psi \to l^+l^-U$. We also calculate the corresponding results for $m_U = \{0.5, 1.0, 1.5, 2.0, 2.5\ \text{GeV}\}$ and list them in Table 4 and Table 5. The predicted event yields at BESIII for the final state l^+l^- + missing mass are at the level of a few events. At STCF, the corresponding yields are $0 \sim 68$ and $0 \sim 63$ for $l = e$ and $l = \mu$, respectively, when the dark photon mass is below 1.3 GeV. In contrast, the event yields for the SM particle final states are all negligible ($\ll 1$).

IV. SUMMARY

We study J/ψ decay processes mediated by the dark photon, which is introduced by an additional $U(1)_Y$ symmetry and kinetically mixes with the photon. The decays considered include two-body channels $J/\psi \to U \to X$ and four-body channels $J/\psi \to l^+l^-U \to l^+l^-X$. The final state X contains only visible SM particles (e^+e^-, $\mu^+\mu^-$, or hadrons) when $m_U < 2m_\chi$. When $m_U \ge 2m_\chi$, X includes both

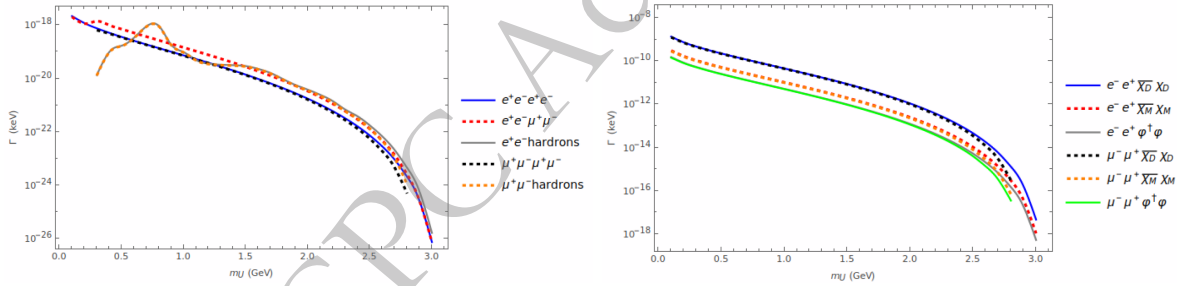

Fig. 10. (color online) Left: Decay width as a function of the dark photon mass m_U for the visible decay processes $J/\psi \to l^+l^-U \to l^+l^-\mu^+\mu^-$, $J/\psi \to l^+l^-U \to l^+l^-e^+e^-$, and $J/\psi \to l^+l^-U \to l^+l^-$hadrons. Right: Decay width as a function of the dark photon mass m_U for the invisible decay processes $J/\psi \to l^+l^-U \to l^+l^-\bar{\chi}_D\chi_D$, $J/\psi \to l^+l^-U \to l^+l^-\bar{\chi}_M\chi_M$, and $J/\psi \to l^+l^-U \to l^+l^-\varphi^\dagger\varphi$, assuming $\alpha_\chi = 0.05$ and $m_U/m_\chi = 3.0$. Both panels correspond to $\epsilon = 10^{-4}$.

Table 3. Predictions for decay ratios $\Gamma/\Gamma_{J/\psi}$ of the four-body decay process $J/\psi \to l^+l^-U \to l^+l^-X$, where X denotes the visible decay products of U, for $m_U < 2m_\chi$ and $m_U = 0.5, 1.0, 1.5, 2.0, 2.5$ GeV. The upper table shows the $J/\psi \to e^+e^-U$ intermediate state, and the lower table shows the $J/\psi \to \mu^+\mu^-U$ intermediate state. The theoretical uncertainty arises entirely from the experimental error in the J/ψ mass. Here, $\epsilon = 10^{-4}$.

	$\mathcal{B}(\times10^{-14})$	$e^+e^-e^+e^-$	$e^+e^-\mu^+\mu^-$	e^+e^-hadrons
$J/\psi \to e^+e^-X$	0.5 GeV	132.990 ± 2.398	131.271 ± 2.367	62.158 ± 1.121
	1.0 GeV	19.969 ± 0.360	19.953 ± 0.360	26.384 ± 0.476
	1.5 GeV	3.0782 ± 0.0555	3.0778 ± 0.0555	6.452 ± 0.116
	2.0 GeV	0.380 ± 0.00685	0.380 ± 0.00685	0.828 ± 0.0149
	2.5 GeV	0.0151 ± 0.000272	0.0151 ± 0.000272	0.0360 ± 0.000649
		$\mu^+\mu^-\mu^+\mu^-$	$\mu^+\mu^-e^+e^-$	$\mu^+\mu^-$hadrons
$J/\psi \to \mu^+\mu^-X$	0.5 GeV	127.531 ± 2.299	129.201 ± 2.329	60.387 ± 1.0886
	1.0 GeV	19.390 ± 0.350	19.405 ± 0.350	25.639 ± 0.462
	1.5 GeV	2.953 ± 0.0532	2.953 ± 0.0532	6.191 ± 0.112
	2.0 GeV	0.350 ± 0.00631	0.350 ± 0.00631	0.763 ± 0.0138
	2.5 GeV	0.0114 ± 0.000206	0.0114 ± 0.000206	0.0273 ± 0.000492

Table 4. Predictions for the decay ratios $\Gamma/\Gamma_{J/\psi}$ of the four-body decay $J/\psi \to l^+l^-U \to l^+l^-X$, where X denotes the visible decay products of U, for $m_U \geq 2m_\chi$ and $m_U = 0.5, 1.0, 1.5, 2.0, 2.5$ GeV. The upper table shows the $J/\psi \to e^+e^-U$ intermediate state, and the lower table shows the $J/\psi \to \mu^+\mu^-U$ intermediate state. The theoretical uncertainty arises entirely from the experimental uncertainty in the J/ψ mass. Here, $\epsilon = 10^{-4}$.

	$\mathcal{B}(\times 10^{-21})$	$e^+e^-e^+e^-$	$e^+e^-\mu^+\mu^-$	e^+e^-hadrons
$J/\psi \to e^+e^-X$	0.5 GeV	3.899 ± 0.0703	3.849 ± 0.0694	1.822 ± 0.0329
	1.0 GeV	0.792 ± 0.0143	0.791 ± 0.0143	1.0465 ± 0.0189
	1.5 GeV	0.151 ± 0.00272	0.151 ± 0.00271	0.316 ± 0.00569
	2.0 GeV	0.0190 ± 0.000342	0.0190 ± 0.00342	0.0413 ± 0.000745
	2.5 GeV	0.000790 ± 0.0000142	0.000790 ± 0.0000142	0.00189 ± 0.0000340
		$\mu^+\mu^-\mu^+\mu^-$	$\mu^+\mu^-e^+e^-$	$\mu^+\mu^-$hadrons
$J/\psi \to \mu^+\mu^-X$	0.5 GeV	3.739 ± 0.0674	3.788 ± 0.0683	1.770 ± 0.0319
	1.0 GeV	0.769 ± 0.0139	0.770 ± 0.0139	1.0170 ± 0.0183
	1.5 GeV	0.144 ± 0.00260	0.145 ± 0.00261	0.303 ± 0.00546
	2.0 GeV	0.0175 ± 0.000315	0.0175 ± 0.000315	0.0381 ± 0.000687
	2.5 GeV	0.000599 ± 0.0000108	0.000599 ± 0.0000108	0.00143 ± 0.0000258

Table 5. Predictions for decay width ratios $\Gamma/\Gamma_{J/\psi}$ for the four-body decay $J/\psi \to l^+l^-U \to l^+l^-X$, where X denotes the invisible decay products of U, for $m_U \geq 2m_\chi$ and $m_U = 0.5, 1.0, 1.5, 2.0, 2.5$ GeV. The upper table corresponds to the $J/\psi \to e^+e^-U$ channel, and the lower table to the $J/\psi \to \mu^+\mu^-U$ channel. The theoretical uncertainty arises entirely from the experimental uncertainty in the J/ψ mass. We set $\epsilon = 10^{-4}$.

	$\mathcal{B}(\times 10^{-14})$	$e^+e^-\bar{\chi}_D\chi_D$	$e^+e^-\bar{\chi}_M\chi_M$	$e^+e^-\varphi^\dagger\varphi$
$J/\psi \to e^+e^-X$	0.5 GeV	243.431 ± 4.388	55.325 ± 0.997	27.663 ± 0.499
	1.0 GeV	49.449 ± 0.891	11.238 ± 0.203	5.619 ± 0.101
	1.5 GeV	9.403 ± 0.170	2.137 ± 0.0385	1.0685 ± 0.0193
	2.0 GeV	1.184 ± 0.0213	0.269 ± 0.00485	0.135 ± 0.00243
	2.5 GeV	0.0493 ± 0.000889	0.0112 ± 0.000202	0.00561 ± 0.000101
		$\mu^+\mu^-\bar{\chi}_D\chi_D$	$\mu^+\mu^-\bar{\chi}_M\chi_M$	$\mu^+\mu^-\varphi^\dagger\varphi$
$J/\psi \to \mu^+\mu^-X$	0.5 GeV	236.495 ± 4.263	53.749 ± 0.969	26.874 ± 0.484
	1.0 GeV	48.0532 ± 0.866	10.921 ± 0.197	5.461 ± 0.0984
	1.5 GeV	9.0216 ± 0.163	2.0504 ± 0.0370	1.0252 ± 0.0185
	2.0 GeV	1.0911 ± 0.0197	0.248 ± 0.00447	0.124 ± 0.00224
	2.5 GeV	0.0374 ± 0.000674	0.00849 ± 0.000153	0.00425 ± 0.0000766

visible SM particles and invisible dark-sector particles (Dirac fermion pairs $\bar{\chi}_D\chi_D$, Majorana fermion pairs $\bar{\chi}_M\chi_M$, or complex scalar pairs $\varphi^\dagger\varphi$). We investigate the influence of the dark photon mass m_U and the kinetic mixing parameter ϵ from two perspectives. For two-body final states, we calculate the decay width as a function of ϵ and present the curves in Figs. 3 and 5 for $m_U = 1.0$ GeV as an example. We also compute the decay width versus m_U and show the results in Figs. 4 and 6 with $\epsilon = 10^{-3}$ chosen as a benchmark, and list the decay ratios $\Gamma/\Gamma_{J/\psi}$ in Tables 1 and 2 for typical masses $m_U = \{0.5, 1.0, 1.5, 2.0, 2.5\ \text{GeV}\}$. The differential transverse momentum distributions $d\sigma/dp_T$ for the $J/\psi \to U \to e^+e^-$ process are displayed in Fig. 7. For four-body final states, we investigate the decay width $\Gamma(J/\psi \to l^+l^-U \to l^+l^-X)$ (see Eq. (14)) divided by ϵ^2 and present the curves in Figs. 8 for $m_U < 2m_\chi$. Meanwhile, for $m_U \geq 2m_\chi$, we study the decay width versus ϵ with $m_U = 1.0$ GeV as an illustration, showing the results in Figs. 9. We also examine the decay width as a function of m_U with $\epsilon = 10^{-4}$ chosen as a benchmark, and present the results in Figs. 10. The corresponding decay ratios $\Gamma/\Gamma_{J/\psi}$ are listed in Tables III and V. All calculations are performed with $\alpha_\chi = 0.05$ and $m_U/m_\chi = 3.0$. We explore the parameter space that can be probed by BESIII and STCF experiments for ϵ and m_U. The detailed analytical formulas are given in Appendix A.

Our results show that, for two-body final states with

$m_U < 2m_\chi$, the expected upper limits on the kinetic mixing parameter ϵ at BESIII are approximately 9.3×10^{-4} and 7.6×10^{-4} for lepton-pair and hadron signals, respectively. The corresponding limits at STCF are 3.7×10^{-4} and 3.1×10^{-4}, respectively. When $m_U \geq 2m_\chi$, for invisible decays, the limit on ϵ is 1.4×10^{-3} for $0.3\ \text{GeV} \leq m_U \leq 0.8\ \text{GeV}$ at BESIII, while the corresponding limit is 2.3×10^{-4} over $0.3\ \text{GeV} \leq m_U \leq 1.9\ \text{GeV}$ at STCF. No signals can be detected for either experiment in other mass regions. For four-body final-state decay channels, signals become undetectable for $m_U < 2.2$ GeV when $\epsilon < 7.6\times10^{-5}$, and no detectable signals exist in the range $2.2\ \text{GeV} \leq m_U \leq 3.0\ \text{GeV}$ at BESIII. For STCF, the corresponding ϵ limit can be pushed down to 1.2×10^{-5} over the entire accessible mass range. When $m_U \geq 2m_\chi$, visible decay channels are nearly excluded at both BESIII and STCF within the theoretical ϵ range. For invisible decays, BESIII yields an ϵ limit of 8.8×10^{-5} for $m_U < 2.4$ GeV, while no signals are detectable for $2.4\ \text{GeV} \leq m_U \leq 3.0\ \text{GeV}$. For STCF, the ϵ limit reaches 1.4×10^{-5} for $m_U < 2.8$ GeV, and no signals can be detected at higher masses. Except for the value 9.3×10^{-4}, the above constraints on ϵ are largely not excluded by current collider experiments. Compared with the limits from two-body final-state processes, the four-body decay channels yield constraints that are considerably lower than current experimental bounds.

Nevertheless, for further phenomenological analysis and better comparison with experimental results, we fix the kinetic mixing parameter to $\epsilon = 10^{-3}$ for two-body decay channels and $\epsilon = 10^{-4}$ for four-body decay channels in our subsequent analysis. The value $\epsilon = 10^{-3}$ has already been excluded by laboratory searches, while $\epsilon = 10^{-4}$ is only ruled out at a few discrete mass points and remains allowed in our considered parameter space [7]. Therefore, our results can serve as an upper bound for two-body decay channels and provide supporting reference for constraining this parameter for BESIII and STCF via four-body decay channels.

ACKNOWLEDGMENTS

We thank Jun Jiang and Wen-Yu Sun for helpful discussions on this work.

APPENDIX A: EXPLICIT FORM OF EXPRESSIONS

In this appendix, we present the explicit analytical expressions used throughout our calculations. Specifically, *a*–*d* correspond to the two-body decay widths of J/ψ; *e* corresponds to $J/\psi \to l^+l^-U$; *f*–*i* correspond to dark photon decays; and *j* corresponds to the differential decay width of $J/\psi \to U \to l^+l^-$.

a. $\Gamma(J/\psi \to U \to l^+l^-)$

$$\frac{64\pi\epsilon^4\alpha^2|\Psi_{J/\psi}(0)|^2\sqrt{M_{J/\psi}^2-4m_l^2}(M_{J/\psi}^2+2m_l^2)}{9M_{J/\psi}[(m_U^2-M_{J/\psi}^2)^2+m_U^2\Gamma_U^2]}. \tag{A1}$$

b. $\Gamma(J/\psi \to U \to \bar{\chi}_D\chi_D)$

$$\frac{64\pi\alpha_\chi\epsilon^2\alpha|\Psi_{J/\psi}(0)|^2\sqrt{M_{J/\psi}^2-4m_\chi^2}(M_{J/\psi}^2+2m_\chi^2)}{9M_{J/\psi}[(m_U^2-M_{J/\psi}^2)^2+m_U^2\Gamma_U^2]}. \tag{A2}$$

c. $\Gamma(J/\psi \to U \to \bar{\chi}_M\chi_M)$

$$\frac{32\pi\alpha_\chi\epsilon^2\alpha|\Psi_{J/\psi}(0)|^2(M_{J/\psi}^2-4m_\chi^2)^{3/2}}{9M_{J/\psi}[(m_U^2-M_{J/\psi}^2)^2+m_U^2\Gamma_U^2]}. \tag{A3}$$

d. $\Gamma(J/\psi \to U \to \varphi^\dagger\varphi)$

$$\frac{16\pi\alpha_\chi\epsilon^2\alpha|\Psi_{J/\psi}(0)|^2(M_{J/\psi}^2-4m_\chi^2)^{3/2}}{9M_{J/\psi}[(m_U^2-M_{J/\psi}^2)^2+m_U^2\Gamma_U^2]}. \tag{A4}$$

e. $\Gamma(J/\psi \to l^+l^-U)$

$$\Gamma(J/\psi \to l^+l^-U) = \frac{1}{2M_{J/\psi}}\int\frac{1}{3}\sum_{\text{spins}}|\mathcal{M}|^2 d\Phi_3, \tag{A5}$$

where the squared amplitude $|\mathcal{M}|^2$ is

$$\begin{aligned}|\mathcal{M}|^2 = {} & 8192\pi^3\epsilon^2\alpha^3|\Psi_{J/\psi}(0)|^2\big(-6m_l^8 \\ & + 2m_U^4(m_l^2-s_2)(m_l^2-s_3)+s_2s_3\big(2M_{J/\psi}^4 \\ & + s_2^2+s_3^2-2M_{J/\psi}^2(s_2+s_3)\big)+m_l^4\big(2M_{J/\psi}^4 \\ & + 3s_2^2+14s_2s_3+3s_3^2-2M_{J/\psi}^2 \\ & (s_2+s_3)\big)-m_l^2\big(-8M_{J/\psi}^2s_2s_3+2M_{J/\psi}^4(s_2+s_3) \\ & + (s_2+s_3)(s_2^2+6s_2s_3 \\ & + s_3^2)\big)+m_U^2\big(2m_l^4(M_{J/\psi}^2-s_2-s_3) \\ & - 2s_2s_3(s_2+s_3)-M_{J/\psi}^2(s_2^2-4s_2s_3 \\ & + s_3^2)-2m_l^2\big(-4s_2s_3+M_{J/\psi}^2(s_2+s_3)\big)\big)\big)/ \\ & 9M_{J/\psi}^3(m_l^2-s_2)^2(m_l^2-s_3)^2.\end{aligned} \tag{A6}$$

f. $\Gamma(U \to l^+l^-)$

$$\frac{\epsilon^2\alpha\sqrt{m_U^2-4m_l^2}(m_U^2+2m_l^2)}{3m_U^2}. \tag{A7}$$

g. $\Gamma(U \to \bar{\chi}_D\chi_D)$

$$\frac{\alpha_\chi \sqrt{m_U^2 - 4m_\chi^2}\,(m_U^2 + 2m_\chi^2)}{3m_U^2}\,. \tag{A8}$$

h. $\Gamma(U \to \bar{\chi}_M \chi_M)$

$$\frac{\alpha_\chi (m_U^2 - 4m_\chi^2)^{3/2}}{6m_U^2}\,. \tag{A9}$$

i. $\Gamma(U \to \varphi^\dagger \varphi)$

$$\frac{\alpha_\chi (m_U^2 - 4m_\chi^2)^{3/2}}{12m_U^2}\,. \tag{A10}$$

j. $d\Gamma(J/\psi \to U \to l^+ l^-)/dp_T$

$$\frac{128\pi\epsilon^4\alpha^2 |\Psi_{J/\psi}(0)|^2 (M_{J/\psi}^2 + 2m_l^2)\,p_T}{9M_{J/\psi}[(m_U^2 - M_{J/\psi}^2)^2 + m_U^2\Gamma_U^2]\sqrt{M_{J/\psi}^2 - 4m_l^2 - 4p_T}}\,. \tag{A11}$$

References

[1] N. Aghanim *et al.* [Planck], "Planck 2018 results. VI. Cosmological parameters," Astron. Astrophys. **641** (2020), A6 [erratum: Astron. Astrophys. **652** (2021), C4] [arXiv: 1807.06209 [astro-ph.CO]].

[2] J. Alexander, M. Battaglieri, B. Echenard, R. Essig, M. Graham, E. Izaguirre, J. Jaros, G. Krnjaic, J. Mardon and D. Morrissey, *et al.* "Dark Sectors 2016 Workshop: Community Report," [arXiv: 1608.08632 [hep-ph]].

[3] M. Battaglieri, A. Belloni, A. Chou, P. Cushman, B. Echenard, R. Essig, J. Estrada, J. L. Feng, B. Flaugher and P. J. Fox, *et al.* "US Cosmic Visions: New Ideas in Dark Matter 2017: Community Report," [arXiv: 1707.04591 [hep-ph]].

[4] P. Agrawal, M. Bauer, J. Beacham, A. Berlin, A. Boyarsky, S. Cebrian, X. Cid-Vidal, D. d'Enterria, A. De Roeck and M. Drewes, *et al.*, Eur. Phys. J. C **81**(11), 1015 (2021), arXiv: 2102.12143[hep-ph]

[5] G. W. Yuan, Z. Q. Shen, Y. L. S. Tsai, Q. Yuan and Y. Z. Fan, Phys. Rev. D **106**(10), 103024 (2022), arXiv: 2205.04970[astro-ph.HE]

[6] M. Fabbrichesi, E. Gabrielli and G. Lanfranchi, "The Dark Photon," [arXiv: 2005.01515 [hep-ph]].

[7] A. Caputo and R. Essig, "The Dark Photon: a 2026 Perspective," [arXiv: 2603.08430 [hep-ph]].

[8] J. P. Lees *et al.* [BaBar], Phys. Rev. Lett. **113**(20), 201801 (2014), arXiv: 1406.2980[hep-ex]

[9] I. Jaegle [Belle], Phys. Rev. Lett. **114**(21), 211801 (2015), arXiv: 1502.00084[hep-ex]

[10] A. Anastasi *et al.* [KLOE-2], Phys. Lett. B **747**, 365 (2015), arXiv: 1501.06795[hep-ex]

[11] S. Abrahamyan *et al.* [APEX], Phys. Rev. Lett. **107**, 191804 (2011), arXiv: 1108.2750[hep-ex]

[12] H. Merkel *et al.* [A1], Phys. Rev. Lett. **106**, 251802 (2011), arXiv: 1101.4091[nucl-ex]

[13] D. Banerjee *et al.* [NA64], Phys. Rev. D **97**(7), 072002 (2018), arXiv: 1710.00971[hep-ex]

[14] Y. M. Andreev *et al.* [NA64], Phys. Rev. Lett. **131**(16), 161801 (2023), arXiv: 2307.02404[hep-ex]

[15] J. P. Lees *et al.* [BaBar], Phys. Rev. Lett. **119**(13), 131804 (2017), arXiv: 1702.03327[hep-ex]

[16] F. Abudinén *et al.* [Belle-II], Phys. Rev. Lett. **130**(7), 071804 (2023), arXiv: 2207.00509[hep-ex]

[17] T. Åkesson *et al.* [LDMX], "Light Dark Matter eXperiment (LDMX)," [arXiv: 1808.05219 [hep-ex]].

[18] P. H. Adrian *et al.* [HPS], Phys. Rev. D **98**(9), 091101 (2018), arXiv: 1807.11530[hep-ex]

[19] P. Ilten, J. Thaler, M. Williams and W. Xue, Phys. Rev. D **92**(11), 115017 (2015), arXiv: 1509.06765[hep-ph]

[20] P. Ilten, Y. Soreq, J. Thaler, M. Williams and W. Xue, Phys. Rev. Lett. **116**(25), 251803 (2016), arXiv: 1603.08926[hep-ph]

[21] B. Aubert *et al.* [BaBar], Phys. Rev. Lett. **103**, 081803 (2009), arXiv: 0905.4539[hep-ex]

[22] J. P. Lees *et al.* [BaBar], Phys. Rev. Lett. **108**, 211801 (2012), arXiv: 1202.1313[hep-ex]

[23] R. Aaij *et al.* [LHCb], Phys. Rev. Lett. **120**(6), 061801 (2018), arXiv: 1710.02867[hep-ex]

[24] R. Aaij *et al.* [LHCb], Phys. Rev. Lett. **124**(4), 041801 (2020), arXiv: 1910.06926[hep-ex]

[25] D. Babusci *et al.* [KLOE-2], Phys. Lett. B **736**, 459 (2014), arXiv: 1404.7772[hep-ex]

[26] D. Babusci *et al.* [KLOE-2], Phys. Lett. B **720**, 111 (2013), arXiv: 1210.3927[hep-ex]

[27] A. Anastasi *et al.* [KLOE-2], Phys. Lett. B **784**, 336 (2018), arXiv: 1807.02691[hep-ex]

[28] A. Hayrapetyan *et al.* [CMS], JHEP **12**, 070 (2023), arXiv: 2309.16003[hep-ex]

[29] S. Navas *et al.* [Particle Data Group], Phys. Rev. D **110**(3), 030001 (2024)

[30] M. Ablikim *et al.* [BESIII], Phys. Rev. D **109**(5), 052006 (2024), arXiv: 2111.13881[hep-ex]

[31] X. R. Lyu [STCF Working Group], PoS **BEAUTY2020**, 060 (2021)

[32] G. T. Bodwin, E. Braaten and G. P. Lepage, Phys. Rev. D **51**, 1125 (1995), arXiv: hep-ph/9407339[hep-ph]

[33] A. Petrelli, M. Cacciari, M. Greco, F. Maltoni and M. L. Mangano, Nucl. Phys. B **514**, 245 (1998), arXiv: hep-ph/9707223[hep-ph]

[34] M. He, X. G. He, C. K. Huang and G. Li, JHEP **03**, 139 (2018), arXiv: 1712.09095[hep-ph]

[35] K. Park, K. Kim, A. Sytov and K. Cho, J. Astron. Space Sci. **40**(4), 259 (2023)

[36] G. Polesello, "Sensitivity of the FCC-ee to the decay of a dark photon into a $\mu^+\mu^-$ pair," [arXiv: 2511.23337 [hep-ph]].

[37] J. Jiang, C. Y. Li, S. Y. Li, S. D. Pathak, Z. G. Si and X. H. Yang, Chin. Phys. C **44**(2), 023105 (2020), arXiv: 1910.07161[hep-ph]

[38] K. Cheung, F. T. Chung and Z. S. Wang, Phys. Rev. D **113**(1), 015013 (2026), arXiv: 2511.02318[hep-ph]

[39] J. Y. Su and J. Tandean, Phys. Rev. D **102**(11), 115029 (2020), arXiv: 2005.05297[hep-ph]

[40] J. Y. Su and J. Tandean, Phys. Rev. D **101**(3), 035044 (2020), arXiv: 1911.13301[hep-ph]

[41] E. Gabrielli, B. Mele, M. Raidal and E. Venturini, Phys.

Rev. D **94**(11), 115013 (2016), arXiv: 1607.05928[hep-ph]
[42] Y. C. San, M. Perelstein and P. Tanedo, Phys. Rev. D **106**(1), 015027 (2022), arXiv: 2205.10304[hep-ph]
[43] T. Hahn, Comput. Phys. Commun. **140**, 418 (2001), arXiv: hep-ph/0012260[hep-ph]
[44] V. Shtabovenko, R. Mertig and F. Orellana, Comput. Phys. Commun. **256**, 107478 (2020), arXiv: 2001.04407[hep-ph]
[45] G. T. Bodwin, D. K. Sinclair and S. Kim, Phys. Rev. Lett. **77**, 2376 (1996), arXiv: hep-lat/9605023[hep-lat]
[46] E. J. Eichten and C. Quigg, Phys. Rev. D **52**, 1726 (1995), arXiv: hep-ph/9503356[hep-ph]
[47] B. Holdom, Phys. Lett. B **166**, 196 (1986)
[48] B. Batell, M. Pospelov and A. Ritz, Phys. Rev. D **80**, 095024 (2009), arXiv: 0906.5614[hep-ph]
[49] R. Essig, J. A. Jaros, W. Wester, P. Hansson Adrian, S. Andreas, T. Averett, O. Baker, B. Batell, M. Battaglieri and J. Beacham, *et al.* "Working Group Report: New Light Weakly Coupled Particles," [arXiv: 1311.0029 [hep-ph]].
[50] G. Krnjaic, "Testing Thermal-Relic Dark Matter with a Dark Photon Mediator," [arXiv: 2505.04626 [hep-ph]].
[51] P. Fayet, Phys. Lett. B **95**, 285 (1980)
[52] P. Fayet, Phys. Rev. D **70**, 023514 (2004), arXiv: hep-ph/0403226[hep-ph]
[53] C. Boehm and P. Fayet, Nucl. Phys. B **683**, 219 (2004), arXiv: hep-ph/0305261[hep-ph]
[54] M. Pospelov, A. Ritz and M. B. Voloshin, Phys. Lett. B **662**, 53 (2008), arXiv: 0711.4866[hep-ph]
[55] B. Batell, M. Pospelov and A. Ritz, Phys. Rev. D **79**, 115008 (2009), arXiv: 0903.0363[hep-ph]
[56] G. Agakishiev *et al.* [HADES], Phys. Lett. B **731**, 265 (2014), arXiv: 1311.0216[hep-ex]
[57] I. Schmidt, E. Bratkovskaya, M. Gumberidze and R. Holzmann, Phys. Rev. D **104**(1), 015008 (2021), arXiv: 2105.00569[hep-ph]
[58] V. V. Anashin *et al.* [KEDR], Phys. Lett. B **788**, 42 (2019), arXiv: 1805.06235[hep-ex]
[59] M. Ablikim *et al.* [BESIII], Chin. Phys. C **46**(7), 074001 (2022), arXiv: 2111.07571[hep-ex]
[60] M. Ablikim *et al.* [BESIII], Phys. Rev. D **88**(3), 032007 (2013), arXiv: 1307.1189[hep-ex]